Georgia Institute of Technology
School of Materials Science and Engineering

Modeling and Simulation of the Impact Response of Linear Cellular Alloys for Structural Energetic Material Applications

By

Adam Jakus
Candidate for Bachelor of Science in Materials Science and Engineering

Undergraduate Thesis
Presented to the Academic Faculty in Partial Fulfillment of Institute Requirements
For the Undergraduate Research Option

Adam Jakus
Undergraduate Student

Dr. Naresh Thadhani
Faculty Advisor
Professor and Associate Chair, School of Materials Science and Engineering

---

David Anthony Fredenburg
Research Mentor
PhD. Candidate, School of Materials Science and Engineering

Dr. Brent Carter
Thesis Review Committee and Undergraduate Chair
Associate Professor, Materials Science and Engineering

Abstract

We investigate the deformation and fracture as well as stress transfer behavior of 250 maraging steel linear cellular alloys (LCAs) undergoing high velocity impact upon a rigid target. Of paramount importance for application as a ballistic delivery mechanism for thermite powders, is the ability to transfer stress along the inner length of the cell walls. Additionally, outward fragmentation of the LCA body upon impact must be controlled. Parameters for a Johnson-Cook strength model of 250 maraging steel are determined in conjunction with 3-dimensional Lagrangian based finite element analysis on a solid cylinder. These parameters are then applied to four, 25% theoretical density LCA geometries: hollow cylinder, pie, reinforced pie, and 9-cell waffle. Verification of the validity of the Johnson-Cook parameters determined from the solid cylinder experiments and simulations is analyzed through comparison of experiments of the four LCA geometries, produced using a direct reduction technique with corresponding simulations. Upon verification of the Johnson-Cook strength model for maraging steel, the deformation and fracture as well as the stress transfer response of the LCAs during impact is analyzed. Through transient analysis of finite element simulations, it has been determined that the 9-cell waffle geometry displays optimal stress transfer behavior as well as limited outward fragmentation.

Table of Contents

1. Introduction

Recent research and applications into metal foams and cellular metals and alloys has focused on their ability to absorb mechanical energy[1-6]. This property results from the porous structure, which provides significant surface area over which mechanical stress can be transmitted. Due to their relatively complex structure, metal foam and cellular metal production has been limited, leading to restricted applications. A direct reduction method (DRM) (Figure 1.1) has recently been developed, to create linear cellular alloys (LCAs), or metallic honey comb structures, of high strength and geometric complexity with relative ease[2]. These LCAs exhibit a unique strength to weight ratio when compressed at high strain rates along their axis[1,5,6]. One potential application for these structures that utilizes their mechanical energy absorption characteristics, is the structural portion of a structural energetic material (SEM). An SEM can be an ideal platform for combined ballistic delivery of chemical and kinetic energies with predictable and conserved deformation and fragmentation upon impact. Current ballistic delivery mechanisms require a significant amount of metallic casing to contain the explosives. The thick casing adds unnecessary weight and also results in significant and often uncontrolled fragmentation upon impact, resulting in collateral damage.

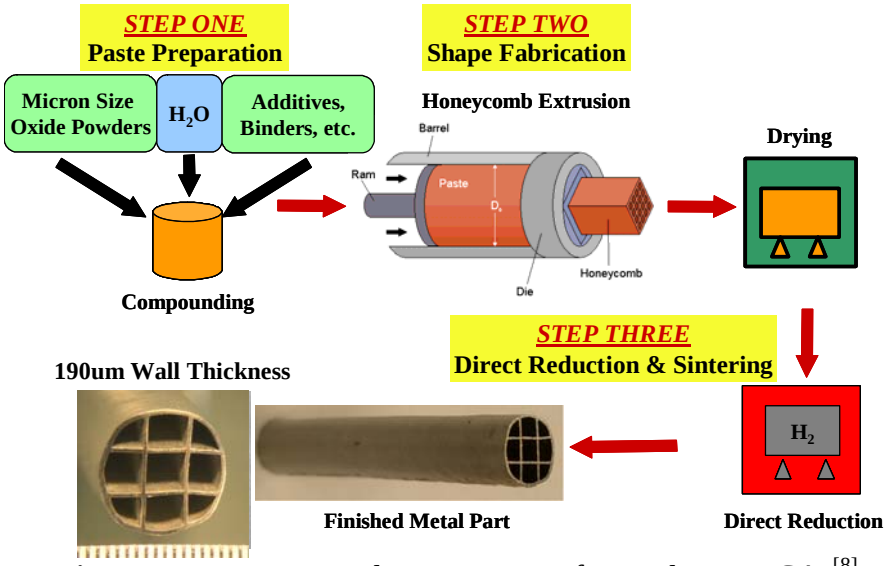

Figure 1.1: Direction reduction process for producing LCAs[8]

Traditionally, metals such as steels display high strength, but no chemical reactivity; an ideal combination for a structural material. Conversely, energetic powder mixtures have high chemical reactivity under certain conditions, but limited strength; an ideal combination for an energetic material. Being both structurally sound and energetically reactive appear to be mutually exclusive material characteristics; however, two materials, one energetic and structurally weak and the other inert and structurally sound, can be coupled to develop a SEM. The projectile, which is composed of a linear cellular alloy made of 250 maraging steel (composition of which can be found in Table 1.1) that provides structural stability, and a reactive powder filler based on a thermite mixture, which provides chemical energy, are coupled to produce the SEM.

Table 1.1: Composition of 250 maraging steel[8]

Element	Weight Percent
C	0.03 max
Mn	0.10 max
Si	0.10 max
P	0.010 max
Si	0.010 max
Ni	17.00-19.00
Co	7.00-8.50
Mo	4.60-5.20
Ti	0.30-0.50
Al	0.05-0.15
Cr	0.50 max
Cu	0.50 max
Fe	Balance

In order accomplish the goal of producing an effective SEM using a 250 maraging steel LCA filled with a reactive powder, an optimal LCA geometry must first be determined that has the following characteristics:

A) Transfers impact-induced stress to the interior cells so as to cause ignition of the powder filler
B) Concentrate kinetic energy at the cross-section of contact over the entire impact duration
C) Undergoes controlled outward fragmentation

To achieve these characteristics and obtain the optimal LCA geometry, a four-fold approach is taken, with each successive step relying on the previous. In this work, we attention is given to steps 1) and 2).

1) Develop an accurate maraging steel Johnson-Cook strength model using simulations based on impact experiments
2) Determine LCA geometry for optimal stress distribution through cell walls
3) Correlate results of simulations and experiments for filled LCA geometries
4) Redefine geometry for optimized strength and reactivity capability

Through understanding of LCA deformation and fracture as well as stress transfer behavior, we hope to make advances towards producing a ballistic delivery mechanism that is both efficient in delivering an energetic payload as well as effective in minimizing collateral damage.

2. Methods and Procedures

Steps 1) and 2) are accomplished through correlation between experimental impact data and simulated impacts using finite element modeling software of solid 250 maraging steel cylinders as well as four pre-determined LCA geometries: hollow cylinder, pie, reinforced pie, and 9-cell waffle, which can be seen in Figure 2.1. All LCAs used for the purposes of this research, both in experiment and simulation, have a similar radius of ~3.8mm and have a theoretical density of ~25% relative to a solid cylinder of the same radius. The ~25% densities and constant radii are maintained through thinning or thickening the cell walls. Experimental 250 maraging steel rods were purchased from Dynamic Metals International and machined to the appropriate initial geometries. The four types of LCAs were produced by Dr. Joe Cochran's group at Georgia Tech using the direct reduction method described earlier.

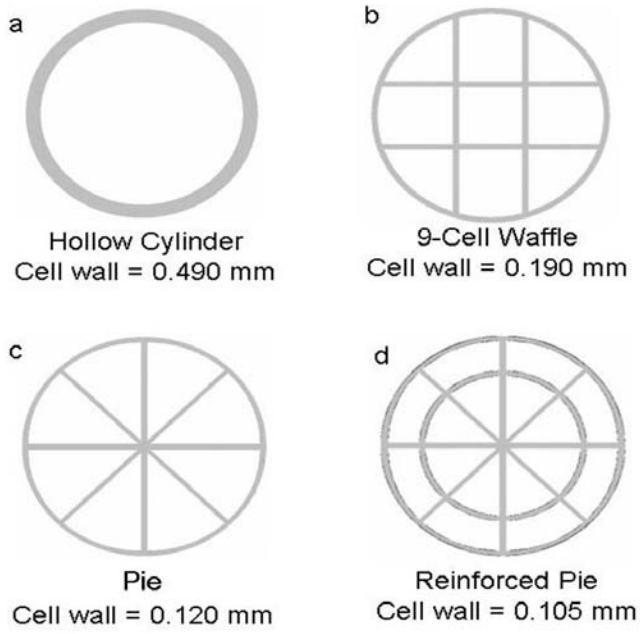

Figure 2.1: LCA geometries and corresponding cell wall thicknesses of a) hollow cylinder b) 9-cell waffle c) pie and d) reinforced pie

Simulations were performed in three dimensions using ANSYS Workbench, a software package containing a CAD-like geometry definition program, a meshing program, and AUTODYN 11.0. A structured Lagrangian mesh was applied to the solid cylinder geometry with 120 cells along its length, 17 along the radial direction and 68 about the circumference (Figure 2.2a). An unstructured Lagrangian mesh was applied to the four LCA geometries of Figure 2.1, an example of which is shown in Figure 2.2b. Boundary conditions were applied to a rigid tungsten anvil to prevent it from moving or deforming upon impact, an appropriate approximation as the mass of the hardened steel anvil used in experiments is orders of magnitude greater than the mass of the impacting cylinders or LCAs. All simulations were run for 50μs simulated time, although in most cases, cylinder or LCA interactions with the anvil ceased at ~30μs. Gauge points that moved with the mesh were placed at locations of interest along the cylinder and LCAs to monitor LCA location, deformation, and pressure (Figure 2.3).

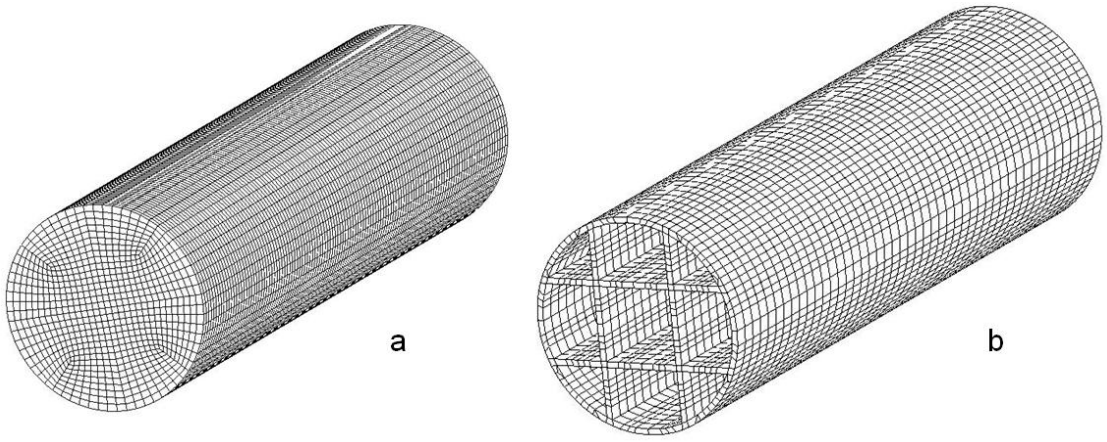

Figure 2.2: Meshing examples for a) solid cylinder and b) 9-cell waffle LCA

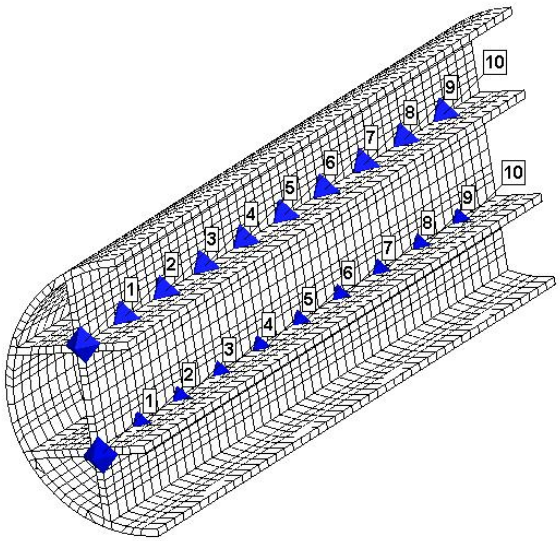

Figure 2.3: Cross-sectional view of 9-cell waffle LCA showing placement of gauge points

2.1 Determination of Accurate 250 Maraging Steel Strength Model

Accomplishing step 1) requires 250 maraging steel impact experiments to calibrate the material model. For this purpose, solid right cylinders of 250 maraging steel are shot from a 7.62mm high velocity gas gun at a rigid steel anvil at 200m/s, with a schematic of the experimental setup shown in Figure 2.4[8]. Velocities are measured using a laser interrupt method and images during impact are then captured using a Hadland Macon 200 high speed digital camera from DRS Technologies. The impacted cylinders are recovered and their dimensions are measured. 3-D simulations are then run using AUTODYN 11.0 with a Lagrangian based finite element solver using initial solid right cylinder geometries and experimental firing conditions. Simulated deformation and fracture properties of the cylinder are controlled through modification of the parameters in a Johnson-Cook strength model (Equation 2.1), with parameter definitions found in Table 2.1[7]. Initial values used for the simulations of these parameters along with other

material parameters can be found in Table 2.2 and were obtained through modification of empirically derived values for steel 4340[7], a similar material to 250 maraging steel.

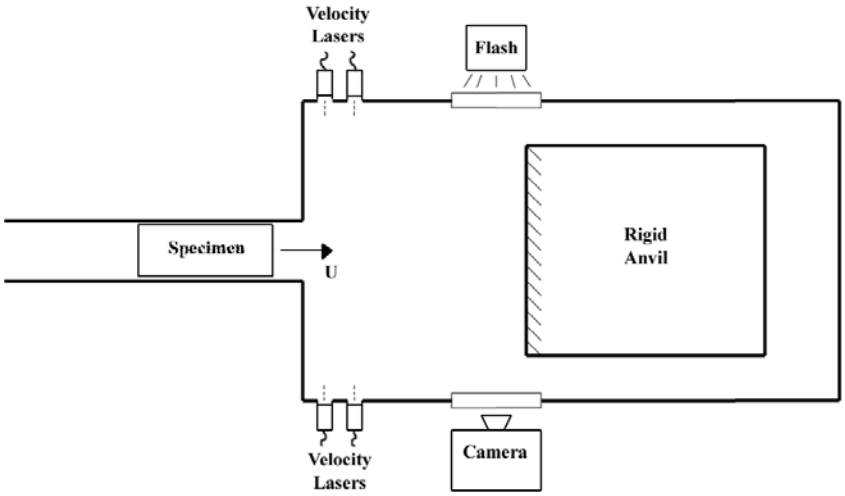

Figure 2.4: Schematic of experimental rod-on-anvil impact test[8]

$$\sigma = \left(A + B\gamma^{n}\right)\left(1 + C\ln\gamma^{*}\right)\left(1 - T^{*^{m}}\right) \tag{2.1}$$

Table 2.1: Variables for Equation 1.1

A =	Static shear strength
B =	Strain-hardening constant
C =	Strain-rate constant
m =	Thermal softening exponent
n =	Strain-hardening exponent
σ =	Flow Stress
γ =	Plastic strain
γ^{*} =	Equivalent plastic strain
T^{*} =	Homologous temperature

Variables *A, B, C, m* and *n* are modified until the simulated transient and final geometries match those of the transient and final geometries of the experimental solid right cylinders impacted at multiple velocities. The simulated geometries' dependence on these parameters is determined through scaling of each parameter individually and

subsequent measurement of simulated post impact geometries. Additional information is obtained through comparisons of transient impact images, captured using a high speed digital camera at 4μs intervals and compared with the simulated transient geometries at the corresponding times. Once optimal values for the Johnson-Cook strength parameters had been determined from solid cylinder geometries, both a hollow cylinder LCA, shot at 155m/s, and a 9-cell waffle LCA, shot at 103m/s, were simulated and the resulting geometry was compared with experiments to further validate the new Johnson-Cook strength parameters.

Table 2.2: Initial material properties used for modeling of 250 maraging steel with properties of interest in bold

Reference Density	7.83	g/cm^3
Equation of State	Linear	
Bulk Modulus	1.59E+08	kPa
Reference Temperature	300	K
Specific Heat	477	J/kgK
Thermal Conductivity	0	J/mKs
Strength Model	Johnson Cook	
Shear Modulus	8.18E+07	kPa
Yield Stress	1.20E+06	kPa
Hardening constant	5.10E+05	kPa
Hardening Exponent	0.26	
Strain Rate Constant	0.014	
Thermal Softening Exponent	1.03	
Melting Temperature	1.79E+03	K
Ref. Strain Rate	1	
Strain Rate Correction	1st Order	
Failure Model	Principal Strain	
Princ. Tensile Failure Strain	0.08	
Max. Princ. Strain Difference / 2	1.01E+20	
Crack Softening	Yes	

2.2 Determination of Optimal LCA Geometry

Upon the determination of values for *A*, *B*, *C*, *m* and *n* using the solid right cylinder experiments and simulations along with further confirmation from the 9-cell waffle LCA experiments and simulations, the previously mentioned Johnson-Cook

parameters were applied to models of the four LCAs and simulated a rigid impact at 200m/s. Their deformation and fragmentation along with stress transfer behavior was observed holding all other simulation parameters constant. Stresses at a given location within the LCA as a function impact time were determined using the attached gauge points and mass loss as a function of impact time was also determined. Fracture behavior was characterized through analysis of the velocity vectors of the cells at and near the impact face.

3. Results

3.1 Solid Cylinder Experiments and Simulations

Simulated solid cylinder impact final lengths and impact face radius as a function of altering a single parameter at a time in the Johnson-Cook model can be seen in Table 3.1 with graphical representations depicted in Figure 3.1. From impact experiments of a solid cylinder of initial length 28.68mm and initial radius 3.77mm at 200m/s, the post impact length was 26.67mm and radius was 5.19mm, or a 7.59% reduction in length and 27.36% increase in radius at the impact face.

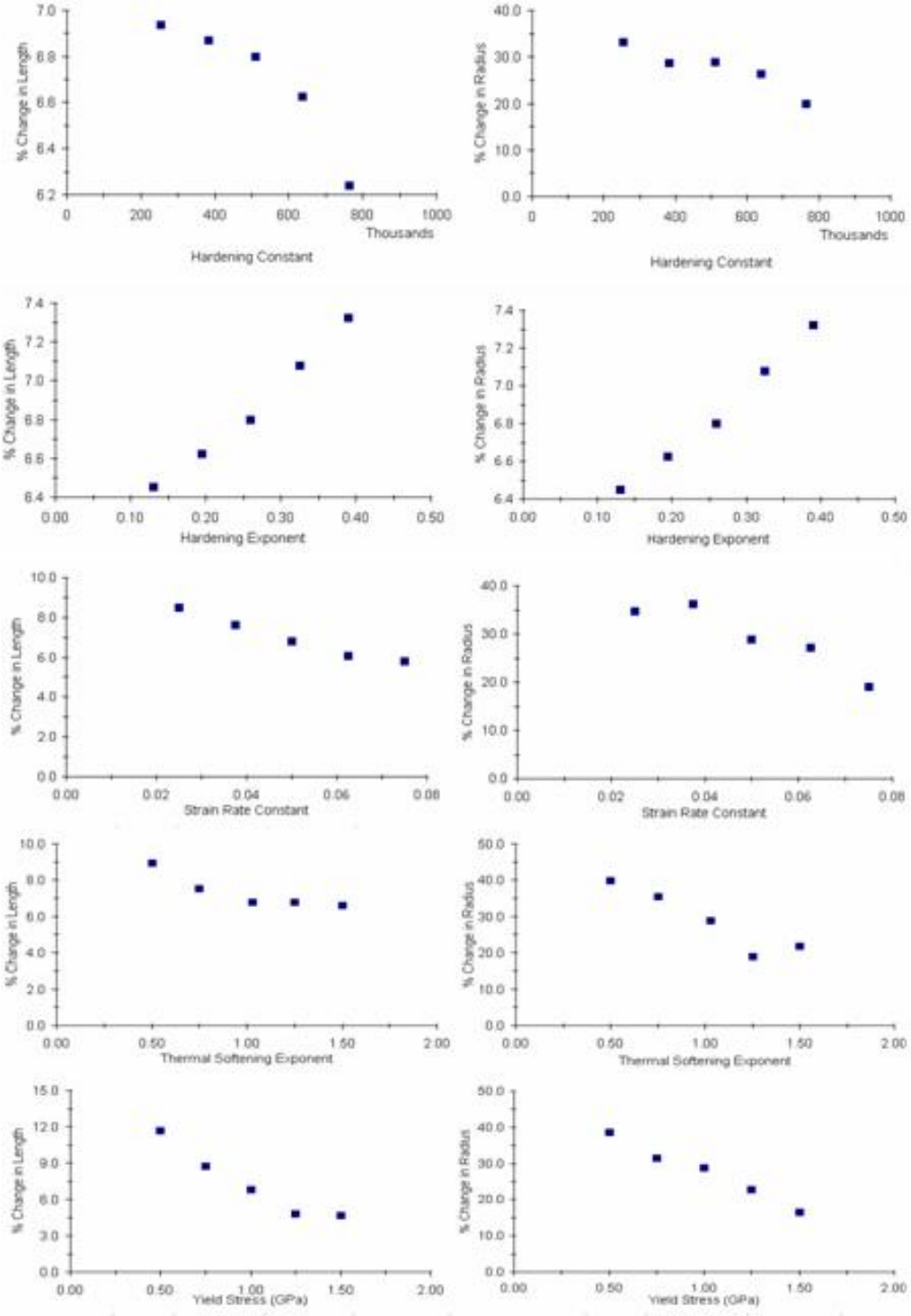

Figure 3.1: Final length and radius as a function of the change in the indicated Johnson-Cook strength parameter

Table 3.1: Geometry property relations for solid cylinder shot at 200m/s. All dimensions are in mm.

	Value	Initial Length	Final Length	Change in Length	% Change in Length	Initial Radius	Final Radius	Change in Radius	% Change in Radius
Hardening Constant	7.65E+05	28.68	26.89	1.79	6.24	3.77	4.70	0.94	19.89
	6.38E+05	28.68	26.78	1.90	6.62	3.77	5.11	1.35	26.32
	5.10E+05	28.68	26.73	1.95	6.80	3.77	5.29	1.53	28.83
	3.83E+05	28.68	26.71	1.97	6.87	3.77	5.28	1.52	28.69
	2.55E+05	28.68	26.69	1.99	6.94	3.77	5.64	1.88	33.24
Hardening Exponent	0.39	28.68	26.58	2.10	7.32	3.77	5.43	1.67	30.66
	0.33	28.68	26.65	2.03	7.08	3.77	5.27	1.51	28.56
	0.26	28.68	26.73	1.95	6.80	3.77	5.29	1.53	28.83
	0.20	28.68	26.78	1.90	6.62	3.77	5.33	1.57	29.36
	0.13	28.68	26.83	1.85	6.45	3.77	5.35	1.59	29.63
Strain Rate Constant	0.08	28.68	27.02	1.66	5.79	3.77	4.65	0.89	19.03
	0.06	28.68	26.94	1.74	6.07	3.77	5.17	1.41	27.18
	0.05	28.68	26.73	1.95	6.80	3.77	5.29	1.53	28.83
	0.04	28.68	26.49	2.19	7.64	3.77	5.90	2.14	36.19
	0.03	28.68	26.24	2.44	8.51	3.77	5.77	2.01	34.75
Thermal Softening Exponent	1.50	28.68	26.79	1.89	6.59	3.77	4.82	1.06	21.89
	1.25	28.68	26.73	1.95	6.80	3.77	4.64	0.88	18.86
	1.03	28.68	26.73	1.95	6.80	3.77	5.29	1.53	28.83
	0.75	28.68	26.52	2.16	7.53	3.77	5.84	2.08	35.53
	0.50	28.68	26.11	2.57	8.96	3.77	6.26	2.50	39.86
Yield Stress	1.50	28.68	27.35	1.33	4.64	3.77	4.51	0.75	16.52
	1.25	28.68	27.30	1.38	4.81	3.77	4.88	1.12	22.85
	1.00	28.68	26.73	1.95	6.80	3.77	5.29	1.53	28.83
	0.75	28.68	26.18	2.50	8.72	3.77	5.50	1.74	31.55
	0.50	28.68	25.33	3.35	11.68	3.77	6.13	2.37	38.58

Through these relationships, the optimal values for the Johnson-Cook strength model were determined and can be found in Table 3.2. Figure 3.2 and Figure 3.3 depict side-by-side half images of the solid cylinder and 9-cell waffle respectively for final simulated and final experimental results. In this instance, the solid cylinder was shot at 200m/s in both experiment and simulation and the 9-cell waffle impacted at 103m/s in both experiment and simulation. Geometrical values pertaining to Figure 3.2 can be found in table 3.3.

Table 3.2: Optimal values for Johnson-Cook strength parameters for 250 maraging steel

A	**1 Gpa**
B	**510 Mpa**
C	**0.05**
m	**1.03**
n	**0.26**

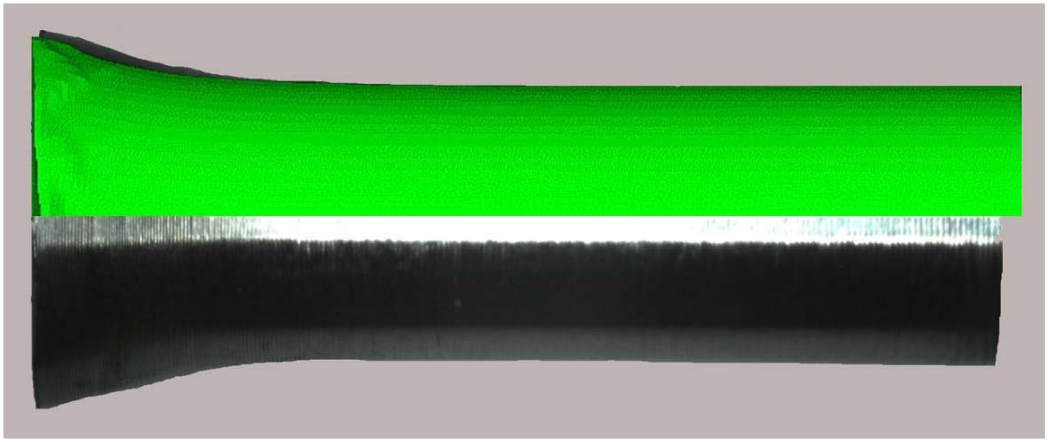

Figure 3.2: Side-by-side images of solid cylinder after simulated (upper) and experimental (lower) impacts at 200m/s

Table 3.3: Relevant geometrical values for Figure 3.2

	Initial Length	Final Length	Initial Radius	Final Radius
Actual	**28.68mm**	**26.67mm**	**3.77mm**	**5.19m**
Simulation	**28.68mm**	**27.1mm**	**3.77mm**	**5.13mm**

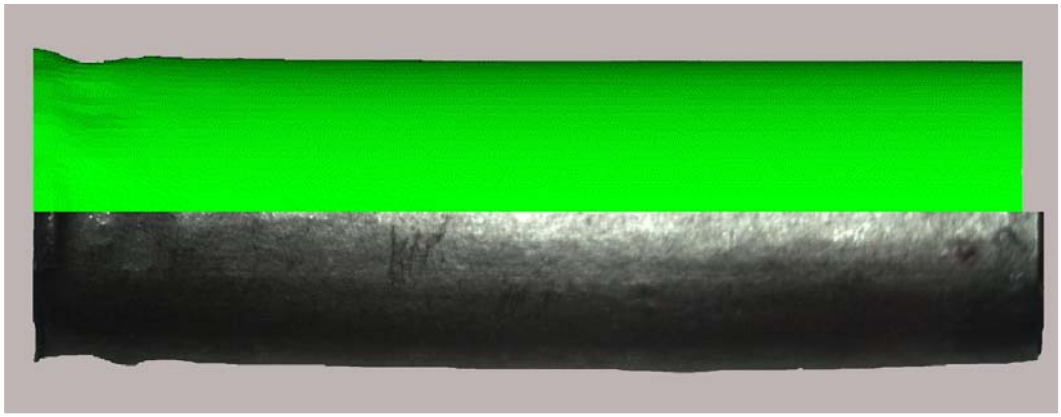

Figure 3.3: Side-by-side images of 9-cell waffle LCA after simulated (upper) and experimental (lower) impacts at 103m/s

Transient images captured by the high speed camera of the solid cylinder impact at 200m/s at 0, 4, 24, and 36μs are shown in Figure 3.4. These images were digitized and the solid cylinder's contours were plotted as function of length and radius. Contour profiles from the experimental impact as well as simulations using a previous 250 Maraging steel model (V250)[9] and the Johnson-Cook model with the values from Table 3.2 are shown in Figure 3.5.

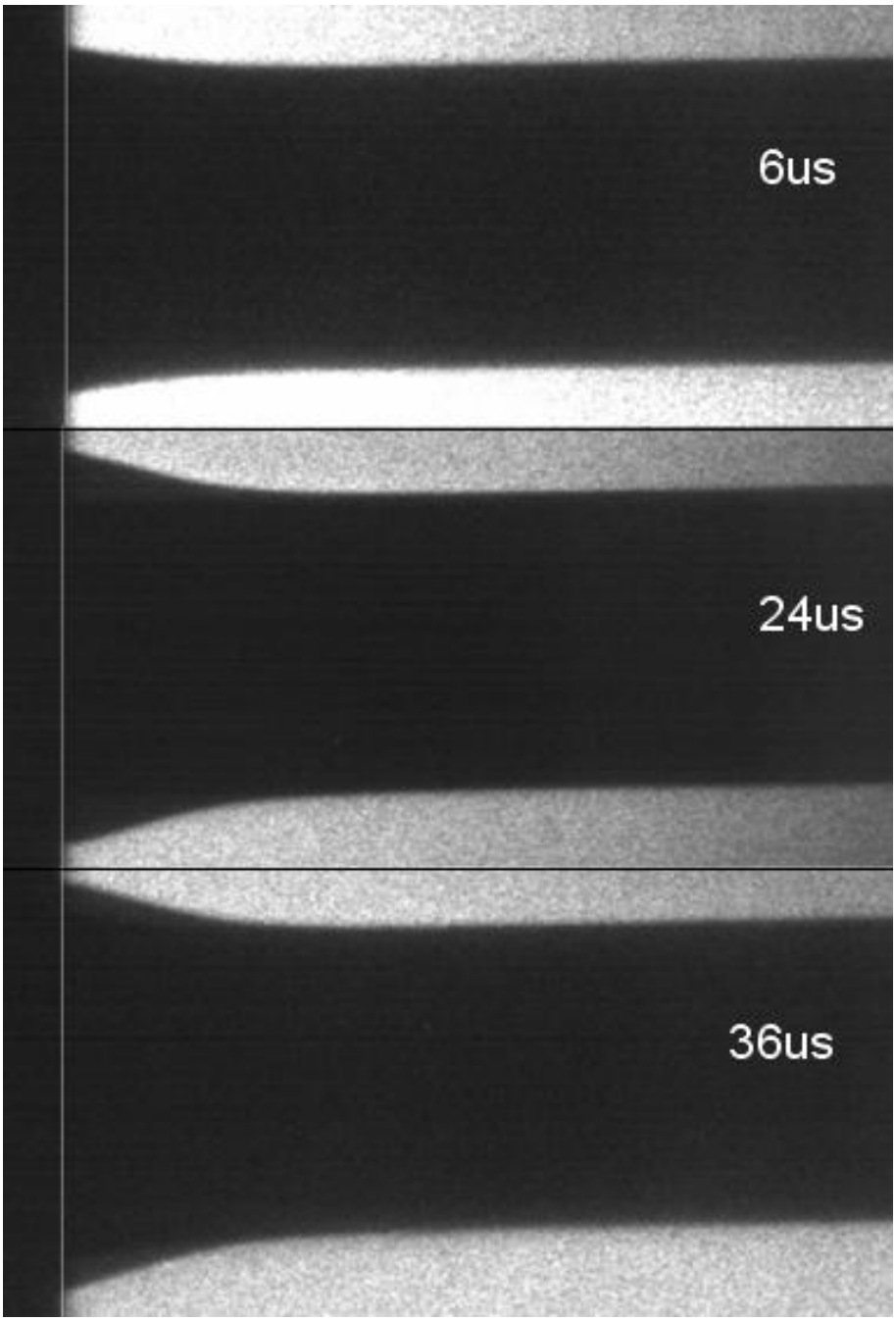

Figure 3.4: Transient images of solid cylinder impact at 6, 24, and 36μs after 200m/s impact on a rigid steel anvil (cylinder/anvil boundary denoted by white line)

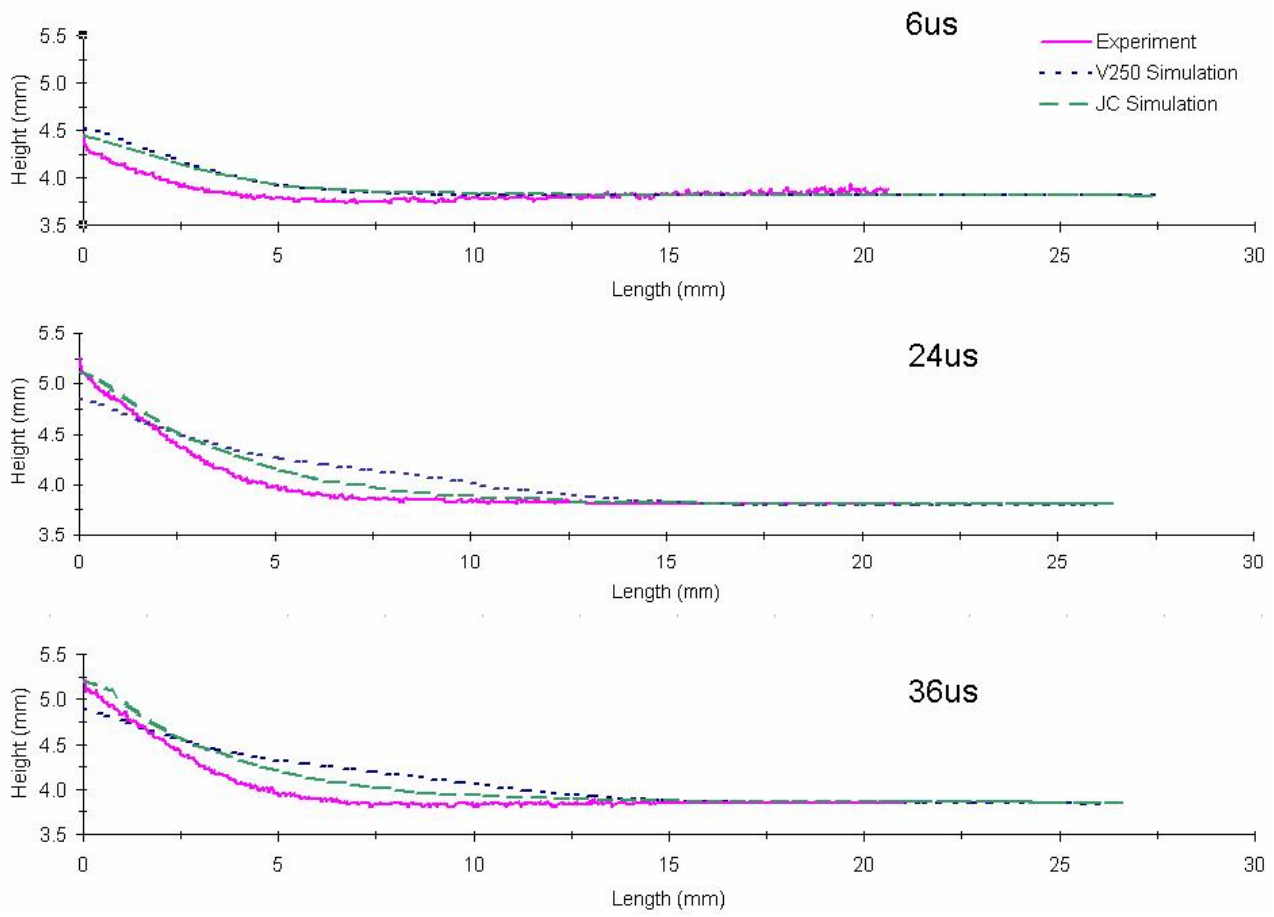

Figure 3.5: Contour plots of solid cylinder impact at 200m/s in experiment and simulations using a preexisting V250 material model[9] and the derived Johnson-Cook material strength model at 6, 24, and 36µs

3.2 Determination of Optimal Geometry

Fragmentation and stress transfer behaviors are characterized for each of the four LCAs impacting at 200 m/s with applied strength model parameters of those determined in *3.1*. The fragmentation nature of a given LCA on impact can be determined by observing the velocity vectors of each of its cells. Figure 3.6 is a graphical representation of the fragmentation behavior of each of the four LCAs captured at 36µs. The arrows' direction indicates the direction of movement of the corresponding cell, and the arrows' color and length are indicative of the magnitude of the cells' velocities.

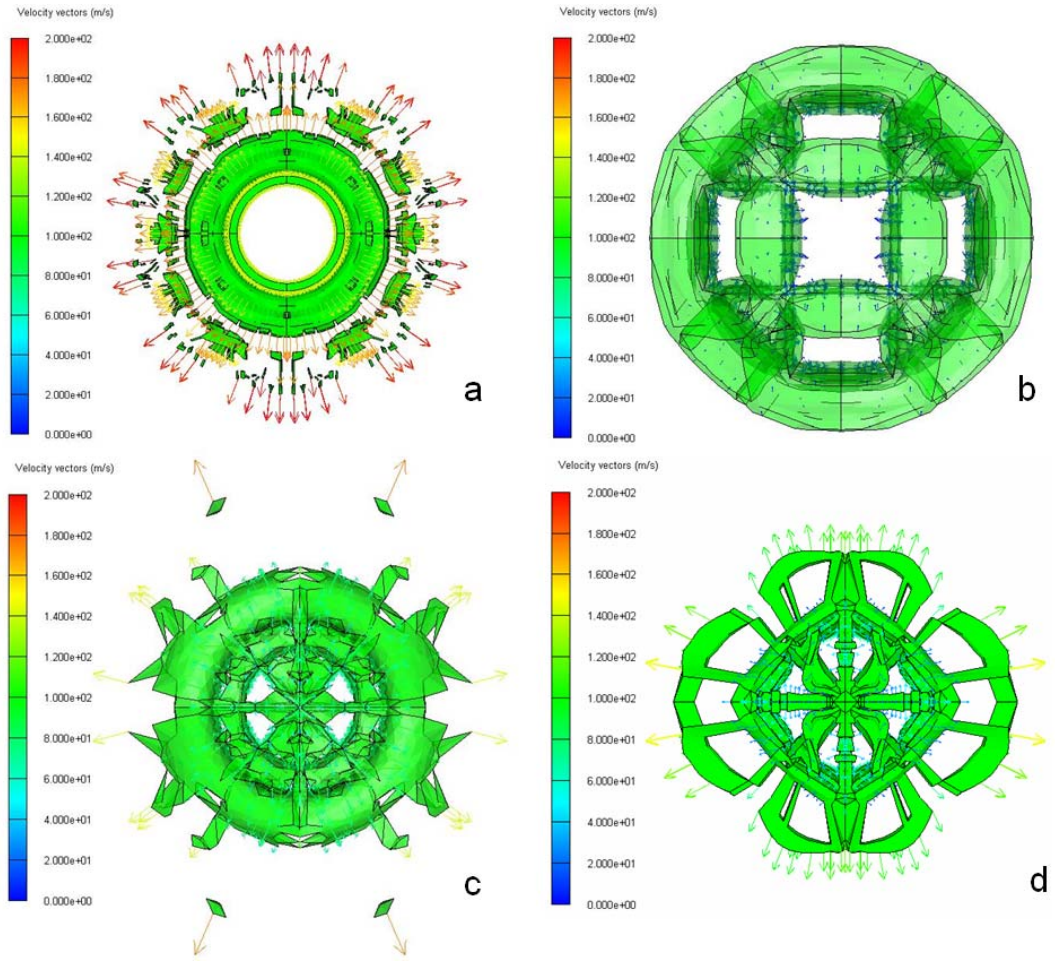

Figure 3.6: Impact face showing material velocity and direction at 36μs of a) hollow cylinder, b) 9-cell waffle, c) reinforced pie, and d) pie. Scale bar is 0-200m/s with 20m/s intervals

Figure 3.7 and Figure 3.8 depict the stress transfer behavior in graphical form as function of distance from the impact face and time, and in pictorial form as a function of time. Stresses at 4mm intervals from the impact face for 20mm were plotted as a function of time. All stress scales in Figure 3.8 are -750MPa to 750MPa with 150MPa intervals where negative values indicate regions of tension and positive values indicate regions of compression.

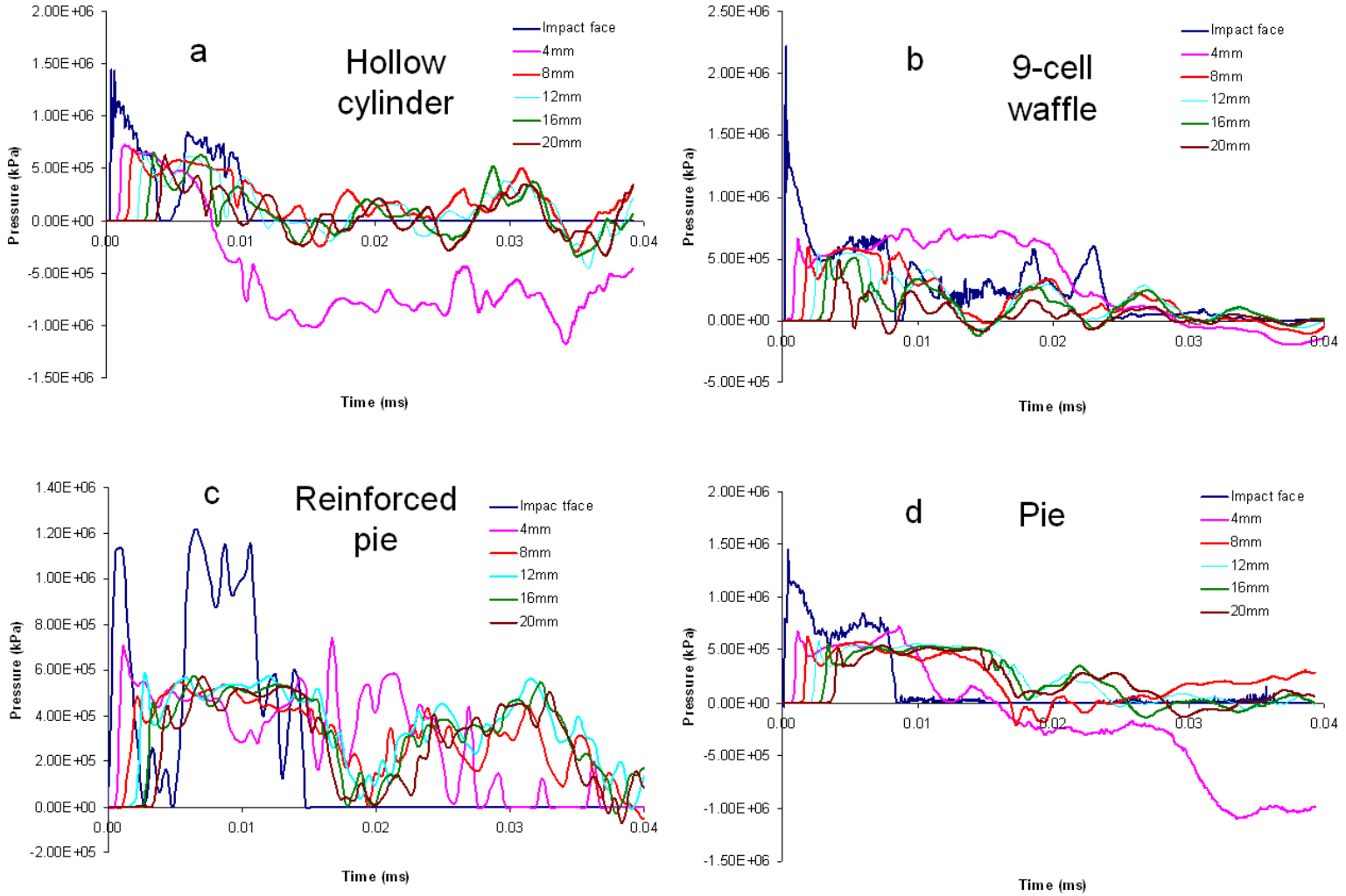

Figure 3.7: Pressure profile along inner LCA walls at 4mm intervals from the impact face as a function of time for a) hollow cylinder b) 9-cell waffle c) reinforced pie and d) pie

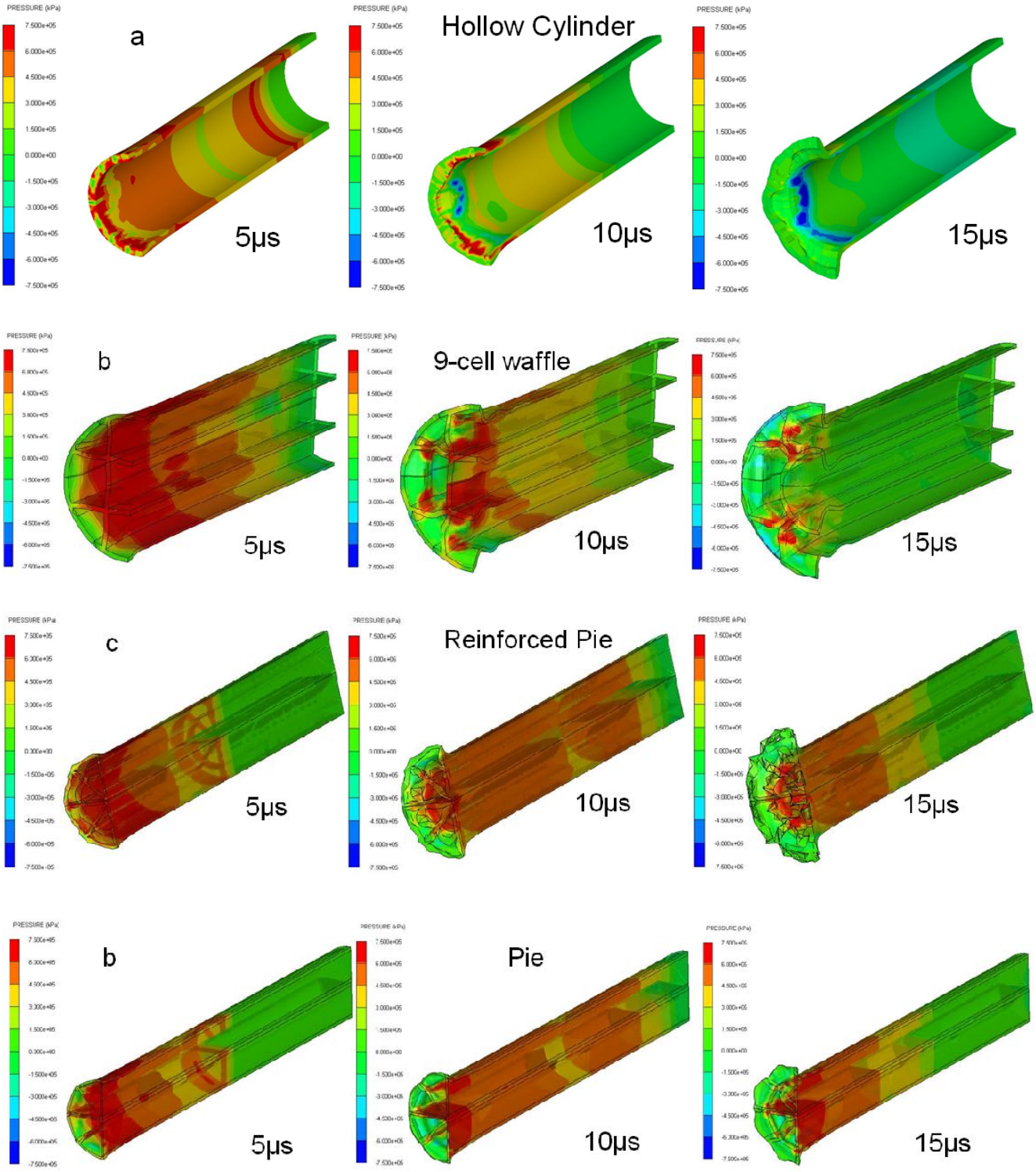

Figure 3.8: Pressure contour images at 5, 10, and 15μs after impact for a) hollow cylinder b) 9-cell waffle c) reinforced pie and d) pie (note that the 9-cell, pie, and reinforced pie have been made semi-transparent to display stresses along inner walls)

4. Analysis

4.1 Solid Cylinder Experiments and Simulations

As indicated by Figure 3.1 and Table 3.1, not all parameters in the Johnson-Cook strength model have equal effect on the flow stress of the material. Small changes in yield strength have significant impact on the final deformation response of the solid cylinder, and consequently, the LCA. As yield strength increases, the change in the LCAs final length and final radius decreases. Alteration of the strain hardening constant has little effect on the final dimensions of the cylinder until a certain threshold is reached between the values of 0.05 and 0.06. Similar to alteration of the yield strength, as the strain hardening constant increases, the change in length and change in radius after impact decreases. Both the strain rate constant and thermal softening exponent show roughly linear but similar trends as changes in the yield strength and hardening constant. Alteration of the strain hardening exponent has very little effect on the final geometry of the cylinder and was found not to be significant in the determination of an accurate strength model for 250 maraging steel.

Through understanding the effects that each of these parameters has on the response of the LCA during impact, an accurate model was developed by reducing the yield strength of the 250 maraging steel to 1GPa and increasing the strain rate constant to 0.05. This modification resulted in a simulated reduction in length of 5.5% and increase in radius of 26.5% as compared with the decrease in length of 7.0% and increase in radius of 27.4% observed from the experimental cylinder shot at 200m/s. Not only are these values relatively close, but Figure 3.2 and Figure 3.3 clearly demonstrate that the simulated profile of the cylinder and 9-cell waffle LCA after impact match those of their experimental counterparts. The derived model is further

validated through transient analysis at multiple times during impact as shown in Figure 3.5. Although the experiment does not completely match with the model parameters determined in this work, the transient final dimensions and profile of the Johnson-Cook modeled simulation have a closer resemblance to the experimental dimensions and profile than the previously accepted 250 Maraging Steel model[9].

4.2 Optimal Geometry

Observation of the simulated LCA deformation and fracture behaviors shown in Figure 3.6 indicate that the hollow cylinder undergoes significant fragmentation upon impact and that those fragments are ejected perpendicular to the axis of impact at velocities comparable to that of the initial, non-fragmented geometry. For purposes of controlled fragmentation and reduction in collateral damage if used as the structural component of an SEM, the hollow cylinder would not be effective. Conversely, the 9-cell waffle shows ideal deformation and fragmentation behavior. Its cell walls fold in upon impact, as indicated by the direction of the velocity vectors. Additionally, at 36μs, most motion within the 9-cell waffle has ceased, unlike within the other LCAs, indicating that the 9-cell efficiently absorbed and dissipated the energy at impact at a greater rate than the others. With regards to optimal fragmentation and deformation response, the 9-cell waffle shows the best results out of the four tested LCAs. Both the pie and reinforced pie display fragmentation behavior between that of the hollow cylinder and 9-cell waffle. In these two geometries, fragments are produced and are ejected outwards, away from the impact site, but there are only several fragments and their velocities are significantly lower than those ejected by the impact of the hollow cylinder.

The analysis of the stress transfer for each LCA upon impact at 200m/s indicates that all four LCAs had initial stresses within the cell walls greater than 1GPa. The 9-cell waffle however has an initial peak stress of 2.25GPa, approximately 750MPa higher than the hollow cylinder and pie and more than 1GPa greater than the reinforced pie. As hypothesized in section *3.1*, and confirmed by the data in Figure 3.7, it appears that the stress in the 9-cell waffle LCA is dissipated at a greater rate than the other three geometries, which all show secondary stress peaks at the impact face. Although the 9-cell waffle exhibits the highest initial stress at the impact face, it has lower stress along its length than any of the other geometries. This may be irrelevant however, as a thermite powder only requires an initial shock and then self-reacts. Taking this fact into consideration, the 9-cell waffle, which has the greatest interior stress at impact, is the optimal geometry with respect to stress transfer behavior.

5. Conclusions

Through variation in the values of individual parameters that make up the Johnson-Cook strength model, an effective material model for 250 maraging steel has been created and successfully applied to impact simulations of 250 maraging steel LCAs of multiple geometries. Fragmentation and stress transfer behavior of each LCA at an impact velocity of 200m/s was analyzed in detail and compared to determine the degree and direction of fragmentation as well as the intensity of stress transfer along the interior walls. Table 5.1 qualitatively summarizes the results of this work.

Table 5.1: Summary of LCA impact behavior

	Fragmentation	**Stress Transfer**
Hollow Cylinder	Very high	High
9-cell waffle	Very low	Very high
Reinforced pie	Moderate	Moderate
Pie	High	High

An ideal LCA for use as the structural component of an SEM should have limited fragmentation to limit collateral damage when used as a ballistic projectile and high interior stress transfer upon impact to ignite the thermite powder payload. Through impact experiments in conjunction with finite element simulations, we have determined that the 9-cell waffle LCA geometry displays optimal behavior in both fragmentation and stress transfer.

6. Acknowledgments

I would like to thank Anthony Fredenburg, Dr. Naresh Thadhani, and the Georgia Tech High Strain-rate Lab for their support, encouragement, and guidance in this work as well as Dr. Joe Cochran's group for producing the LCAs. I would also like to acknowledge the funding received for this research from the Homeland Defense Threat Reduction Agency Grant No.: HDTRA1-07-1-0018 and for me personally through President's Undergraduate Research Awards.

7. References

[1] A.M. Hayes, A. Wang, B.M. Dempsey, D.L. McDowell, "Mechanics of linear cellular alloys,"Mechanics of Materials, vol. 36, pp. 691-713, 2003.

[2] J. Cochran, K.J. Lee, D. McDowell, T.H. Sanders, et al., "Low density monolithic metal honeycombs by thermal chemical processing.,"4th Conference on Aerospace Materials, Processes, and Environmental Technology, September, 2000.

[3] M.F. Ashby, A. Evans, N.A. Fleck, L.J. Gibson, J.W. Hutchinson, H.N.G. Wadley, Metal Foams - A Design Guide, Boston: Butterworth-Heinemann, 2000.

[4] F.P. Incropera and D.P. DeWitt, Fundamentals of Heat and Mass Transfer, 4th ed., New York: John Wiley and Sons, 1996.

[5] A. Hayes, Compression Behavior of linear cellular steel, M.S. Thesis. , Atlanta: Georgia Institute of Technology, 2001.

[6] E. Wu and W. Jiang, "Axial crushing of metallic honeycombs, "International Journal of Impact Engineering, vol. 19, no. 5-6, pp. 439-456, 1997.

[7] G.R. Johnson and W.H. Cook, “A Constitutive Model and Data for Metals Subjected to Large Strains, High Strain Rates and High Temperatures,” Honeywell Inc. Defense Systems Division, Hopkins, Minnesota and Air Force Armament Laboratory Eglin Air Force Base, Florida.

[8] D. Anthony Fredenburg, “LCA Report for Dr. Naresh Thadhani: 2008,” Georgia Tech. 2008.

[9] D.J. Steinberg "Equation of State and Strength Properties of Selected Materials". LLNL. Feb 1991